Implementation and efficiency of several geometric stiffening approaches

J. Cuadrado*
University of La Coruña
Ferrol, Spain

U. Lugrís†
University of La Coruña
Ferrol, Spain

Abstract— *The floating frame of reference formulations are widely used for the modelling of flexible bodies in multibody systems. In the particular case of beams, the geometric stiffening effect is often lost due to the assumption of linear elastic forces. This paper discusses the implementation of different existing methods developed to consider such geometric nonlinearities within a floating frame of reference formulation, making emphasis on the relation between efficiency and accuracy of the resulting algorithms, seeking to provide practical criteria of use.*

Keywords: flexible, multibody, geometric stiffening

I. Introduction

One of the most common methods of flexible body modelling in multibody systems is the floating frame of reference approach (FFR) [1], in which a local frame of reference is attached to the flexible body, so that the elastic deformation is measured in the local frame and superimposed to the large amplitude motion, undergone by the reference frame. Small deformation theory is applied and, therefore, it cannot be used in large deformation problems. In specific applications, such as helicopter rotor blades, the stiffening effect appears due to the geometrical nonlinearity. Helicopter rotor blades are bent by their own weight, but the rotation speed makes them rise up to the horizontal position, due to centrifugal forces, as if the bending stiffness increased [2], [3], [4], [5]. In a linear model, this effect is not captured due to the absence of coupling between axial and transversal deformation, which implies that rotational speed has no effect on bending, but only on the radial displacement.

There exist several techniques aimed to include this effect in beams. In this paper, the implementation of two of them in a FFR formulation is described, and the results are compared to those obtained with a global, finite element based, nonlinear formulation, the ANCF [1], [6].

II. The Specific FFR Formulation

The equations of motion, according to an index-3 augmented Lagrangian formulation in natural dependent coordinates [7], are stated in the form,

$$\mathbf{M}\ddot{\mathbf{q}} + \mathbf{\Phi}_{\mathbf{q}}^T \alpha \mathbf{\Phi} + \mathbf{\Phi}_{\mathbf{q}}^T \boldsymbol{\lambda}^* = \mathbf{Q} \tag{1}$$

where $\mathbf{q}$ is the vector of natural coordinates, $\mathbf{M}$ is the mass matrix, $\mathbf{\Phi}, \mathbf{\Phi}_{\mathbf{q}}$ are the constraints vector and its Jacobian matrix, $\mathbf{Q}$ is the vector of elastic, applied and velocity-dependent inertia forces, and $\boldsymbol{\lambda}^*$ is the Lagrange multipliers vector, obtained from an iterative process carried out within each time-step,

$$\boldsymbol{\lambda}_{i+1}^* = \boldsymbol{\lambda}_i^* + \alpha \mathbf{\Phi}_{i+1} \qquad i = 0,1,2,... \tag{2}$$

which starts with $\boldsymbol{\lambda}_0^*$ equal to the value of $\boldsymbol{\lambda}^*$ obtained in the previous time-step. These equations are integrated in time by means of a Newmark-type integrator, along with velocity and acceleration projections at the end of each time-step to preserve stability [7].

The case of a planar flexible beam is to be described for the sake of simplicity. However, the procedure can be generalized to the 3D case.

The considered FFR approach defines the deformation of a flexible planar beam in a local reference frame, which is attached to a material point of the beam and undergoes the large amplitude rigid-body motion. The position $\mathbf{r}$ of any point of the solid can be expressed as,

$$\mathbf{r} = \mathbf{r}_0 + \mathbf{A}\left(\bar{\mathbf{r}}_u + \boldsymbol{\delta}\right) \tag{3}$$

where $\mathbf{r}_0$ is the position of the local frame origin, $\mathbf{A}$ the rotation matrix defined by the two orthogonal local unit vectors $\left[\mathbf{u} \mid \mathbf{v}\right]$, $\bar{\mathbf{r}}_u$ the undeformed position in local coordinates, and $\boldsymbol{\delta}$ the local elastic displacement.

Using the finite element method to discretize the beam with 2D beam elements, the neutral axis displacement within a finite element e, $\boldsymbol{\delta}_0^e$, can be interpolated from its nodal displacements, $\mathbf{q}_f^e$, by means of the interpolation matrix, $\mathbf{S}^e$, which can be split into longitudinal and transversal interpolation submatrices, $\mathbf{S}_l^e$ and $\mathbf{S}_t^e$,

$$\boldsymbol{\delta}_0^e = \begin{pmatrix} u_0 \\ v_0 \end{pmatrix} = \mathbf{S}^e \mathbf{q}_f^e = \begin{pmatrix} \mathbf{S}_l^e \\ \mathbf{S}_t^e \end{pmatrix} \mathbf{q}_f^e \tag{4}$$

where u_0 and v_0 are the local components of $\boldsymbol{\delta}_0^e$.

The dimension of the finite element model is reduced by using component mode synthesis, in this case a Craig-Bampton reduction, with static and dynamic modes [7], [9]. This reduction consists of approximating the vector of

* E-mail: javicuad@cdf.udc.es
† E-mail: ulugris@udc.es

nodal displacements by means of a linear combination of *ns* static modes $\mathbf{\Phi}_i$ and *nd* dynamic modes $\mathbf{\Psi}_j$,

$$\mathbf{q}_f = \sum_{i=1}^{ns} \mathbf{\Phi}_i \eta_i + \sum_{j=1}^{nd} \mathbf{\Psi}_j \xi_j \tag{5}$$

where $\mathbf{q}_f$ is a vector grouping all the nodal displacements of the beam, and the coefficients η_i and ξ_j are the modal amplitudes. This can be written in a more compact matrix form,

$$\mathbf{q}_f = \begin{bmatrix} \mathbf{\Phi}_1 & \cdots & \mathbf{\Phi}_{ns} & \mathbf{\Psi}_1 & \cdots & \mathbf{\Psi}_{nd} \end{bmatrix} \begin{Bmatrix} \eta_1 \\ \vdots \\ \eta_{ns} \\ \xi_1 \\ \vdots \\ \xi_{nd} \end{Bmatrix} = \mathbf{X}\mathbf{y} \tag{6}$$

Compatibility constraints must be added in order to relate the amplitudes of the static modes to the corresponding joint displacements. Finally, the vector of variables for a single flexible beam results,

$$\mathbf{q} = \begin{Bmatrix} \mathbf{r}_0 & \mathbf{u} & \mathbf{v} & \eta_1 & \cdots & \eta_{ns} & \xi_1 & \cdots & \xi_{nd} \end{Bmatrix}^T \tag{7}$$

With all the flexible body kinematics defined, the mass matrix can be calculated. The elastic displacement can be particularized to node *i* as $\boldsymbol{\delta}_0^i = \mathbf{q}_f^i = \mathbf{X}^i\mathbf{y}$, being $\mathbf{X}^i$ the couple of rows of $\mathbf{X}$ corresponding to the longitudinal and transversal displacements of node *i*. The absolute velocity of node *i*, $\mathbf{v}_i$, can be calculated by substituting its elastic displacement in Eq. (3), and differentiating with respect to time,

$$\mathbf{v}^i = \dot{\mathbf{r}}_0 + \dot{\mathbf{A}}\left(\overline{\mathbf{r}}_u^i + \mathbf{X}^i\mathbf{y}\right) + \mathbf{A}\mathbf{X}^i\dot{\mathbf{y}} \tag{8}$$

The co-rotational approximation [7], [8], consists of interpolating the velocity of any given point inside a finite element from the velocities of its nodes, through the displacement interpolation matrix $\mathbf{S}^e$. Accordingly, the kinetic energy can be written in terms of the nodal velocities $\mathbf{v}$ and the finite element mass matrix $\mathbf{M}_{FEM}$,

$$T = \frac{1}{2}\int_V \dot{\mathbf{r}}^T\dot{\mathbf{r}}dm = \frac{1}{2}\int_V \mathbf{v}^T\mathbf{S}^T\mathbf{S}\mathbf{v}dm = \frac{1}{2}\mathbf{v}^T\mathbf{M}_{FEM}\mathbf{v} \tag{9}$$

where $\mathbf{S}$ contains the assembled interpolation matrices of all the finite elements of the flexible body. Eq. (8) can be written in matrix form for all the nodes, since it is linear with respect to the generalized velocities $\dot{\mathbf{q}}$,

$$\mathbf{v} = \mathbf{B}(\mathbf{q})\dot{\mathbf{q}} \tag{10}$$

Finally, this relationship can be substituted into Eq. (9) to obtain the mass matrix,

$$\mathbf{M} = \mathbf{B}^T\mathbf{M}_{FEM}\mathbf{B} \tag{11}$$

Velocity-dependent inertia forces $\mathbf{Q}_v = -\mathbf{B}^T\mathbf{M}_{FEM}\dot{\mathbf{B}}\dot{\mathbf{q}}$ must be added to the generalized forces vector $\mathbf{Q}$. The calculation of the elastic forces will be addressed in the following section.

III. Geometric Nonlinearity Consideration

The elastic displacements field $\boldsymbol{\delta}(x,y)$ of an Euler-Bernoulli beam takes the following vector form [5],

$$\boldsymbol{\delta}(x,y) = \begin{bmatrix} u \\ v \end{bmatrix} = \begin{bmatrix} u_0 - yv_0' \\ v_0 \end{bmatrix} \tag{12}$$

where u_0 and v_0 are the axial and transversal displacements of the neutral axis, and the apostrophe indicates differentiation with respect to the *x* coordinate. The nonlinear strain-displacement relationship in *x* direction can be expressed as,

$$\varepsilon_{xx} = u' + \frac{1}{2}\left[(u')^2 + (v')^2\right] \cong u' + \frac{1}{2}(v')^2 \tag{13}$$

where the term $(u')^2$ is often dropped since it is much smaller than u'. The elastic potential of the beam depends on this strain field,

$$U = \frac{1}{2}\int_V E\varepsilon_{xx}^2 dV \tag{14}$$

where *E* is the Young modulus and *V* is the volume of the beam. Introduction of the displacement field described by Eq. (12) in the strain-displacement relationship, yields the deformation energy of the beam in terms of the neutral axis deformed shape [5],

$$\begin{aligned} U = &\underbrace{\frac{1}{2}\int_0^L EA(u_0')^2\,dx + \frac{1}{2}\int_0^L EI(v_0'')^2\,dx}_{\text{Linear formulation}} + \\ &+ \underbrace{\frac{1}{2}\int_0^L EAu_0'(v_0')^2\,dx}_{\text{First nonlinear formulation}} + \underbrace{\frac{1}{8}\int_0^L EA(v_0')^4\,dx}_{\text{Second nonlinear formulation}} \end{aligned} \tag{15}$$

with *A* the cross-sectional area and *I* the second moment of area with respect to the neutral axis.

Different levels of approximation can be achieved depending on which terms of Eq. (15) are kept: they are

discussed in the following sub-sections.

A. *Linear formulation*

The linear formulation includes only the first two terms of Eq. (15) in the elastic potential, neglecting the higher order ones. Introducing the finite element discretization in the equation and integrating the interpolation functions, the following expression can be obtained for the elastic potential in terms of the finite element coordinates,

$$U = \frac{1}{2}\mathbf{q}_f^T \mathbf{K}_L^{FEM} \mathbf{q}_f \tag{16}$$

Here, $\mathbf{K}_L^{FEM}$ is the linear stiffness matrix, which is constant, and $\mathbf{q}_f$ is a vector containing the nodal displacements of the whole beam. This potential can be projected to the modal base by using matrix **X**,

$$U = \frac{1}{2}\mathbf{y}^T \mathbf{X}^T \mathbf{K}_L^{FEM} \mathbf{X}\mathbf{y} = \frac{1}{2}\mathbf{y}^T \mathbf{K}_L \mathbf{y} \tag{17}$$

By differentiation of the elastic potential, an expression for the elastic forces is obtained,

$$\mathbf{F}_{el} = -\left(\frac{\partial U}{\partial \mathbf{y}}\right)^T = -\mathbf{K}_L \mathbf{y} \tag{18}$$

which is a linear relationship between the forces and the modal amplitudes. A closer look to the potential used in this formulation reveals the cause of its inability to capture geometric stiffening effects: axial and transversal displacements separately contribute to the deformation energy.

B. *First nonlinear formulation*

When the third term of Eq. (15) is considered too, the coupling between axial and transversal deformation is introduced through the integral of $u_0'\left(v_0'\right)^2$. This allows to capture the geometric stiffening effect, at the cost of a non-constant stiffness matrix, as it will be shown below.

The same steps as in the linear formulation must be carried out to obtain the elastic potential: the u_0 and v_0 derivatives are substituted by their finite element interpolations, and the integrals are evaluated; then, writing it in matrix form [3], [4],

$$U = \frac{1}{2}\mathbf{q}_f^T \left(\mathbf{K}_L^{FEM} + \mathbf{K}_G^{FEM}\right)\mathbf{q}_f \tag{19}$$

The geometric stiffness matrix $\mathbf{K}_G^{FEM}$ is variable, and must be calculated at every time-step. In case that the axial displacement u_0 has a linear distribution, the strain is constant along the whole beam, and $\mathbf{K}_G^{FEM}$ can be expressed as the product of a scalar variable times a constant matrix. But in any other case, this is only applicable to each finite element, and the matrix must be assembled at every time-step, which is rather inefficient.

It is better to express u_0 and v_0 in terms of the mode shapes and then carry out the spatial integration. First, the neutral axis displacements are approximated by the modal superposition,

$$\begin{aligned} u_0(x) &= \sum_{i=1}^{ns} \phi_l^i(x)\eta_i + \sum_{j=1}^{nd} \psi_l^j(x)\xi_j \\ v_0(x) &= \sum_{i=1}^{ns} \phi_t^i(x)\eta_i + \sum_{j=1}^{nd} \psi_t^j(x)\xi_j \end{aligned} \tag{20}$$

where the subindices *l* and *t* indicate longitudinal or transversal component, respectively. These approximated displacements are then used to calculate the integral. The analytical functions of the mode shapes are usually known for a beam and, therefore, they can be directly integrated. In the case that the modes are finite element displacement vectors, integrals must be calculated by using the interpolation functions. The geometric stiffness matrix, already projected to the modal subspace, takes the following linear combination form,

$$\mathbf{K}_G = \sum_{i=1}^{ns} \eta_i \mathbf{K}_G^i + \sum_{i=1}^{nd} \xi_j \mathbf{K}_G^j \tag{21}$$

where all the $\mathbf{K}_G^i$ and $\mathbf{K}_G^j$ matrices are constant, and have the form,

$$\mathbf{K}_G^i = \int_0^L EA\phi_l'^i \begin{Bmatrix} \phi_t'^1 \\ \vdots \\ \phi_t'^{ns} \\ \psi_t'^1 \\ \vdots \\ \psi_t'^{nd} \end{Bmatrix} \begin{Bmatrix} \phi_t'^1 & \cdots & \phi_t'^{ns} & \psi_t'^1 & \cdots & \psi_t'^{nd} \end{Bmatrix} dx \tag{22}$$

with $\psi_l'^j$ instead of $\phi_l'^i$ for $\mathbf{K}_G^j$. These matrices are nonzero for mode *i* or *j* only if the mode is longitudinal, so that there is one nonzero matrix for each axial mode.

Differentiation of the elastic potential with respect to **y**, neglecting the term which contains the derivative of $\mathbf{K}_G$, yields the elastic forces vector,

$$\mathbf{F}_{el} = -\left(\frac{\partial U}{\partial \mathbf{y}}\right)^T = -\left(\mathbf{K}_L + \mathbf{K}_G\right)\mathbf{y} \tag{23}$$

The modifications needed to implement this in the formulation are minimal. First, all the integrals of Eq. (22)

must be calculated, thus obtaining one constant matrix for each axial mode. Then the $\mathbf{K}_G$ matrix is computed at every time-step by using Eq. (21) and added to $\mathbf{K}_L$ to obtain the elastic forces.

C. *Second nonlinear formulation*

In this formulation, the four terms of the elastic energy in Eq. (15) are considered, being the most suitable for severe deformation conditions but, logically, at the cost of a higher computational effort.

$$U = \frac{1}{2}\mathbf{q}_f^T \left(\mathbf{K}_L^{FEM} + \mathbf{K}_G^{FEM} + \mathbf{K}_H^{FEM}\right)\mathbf{q}_f \qquad (24)$$

The inclusion of the higher order term adds a second-order nonlinear matrix $\mathbf{K}_H^{FEM}$, and the elastic forces are obtained by differentiation,

$$\mathbf{F}_{el} = -\left(\frac{\partial U}{\partial \mathbf{q}_f}\right)^T = -\left(\mathbf{K}_L^{FEM} + \mathbf{K}_G^{FEM} + \mathbf{K}_H^{FEM}\right)\mathbf{q}_f + \mathbf{Q}_g \qquad (25)$$

where all the terms depending on the derivatives of the non-constant **K** matrices are grouped into the generalized nonlinear forces vector $\mathbf{Q}_g$. The main problem of this formulation is that it needs a high number of axial modes to obtain accurate results [3], [4], making its use impractical.

D. *Foreshortening formulation*

The axial shortening of a beam due to its deflection is known as *foreshortening* (figure 1).

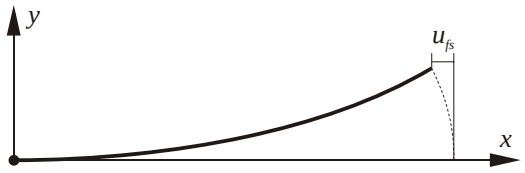

Fig. 1. Foreshortening produced by deflection.

This effect cannot be captured by using the linear or nonlinear formulations. The explicit inclusion of the foreshortening effect in the model leads to a simpler and more efficient method [3], [4], and provides the same level of accuracy as the second nonlinear formulation.

The axial displacement of the neutral axis can be divided into the axial deformation produced by the actual axial forces, *s*, and the shortening produced by the deflection u_{fs}

$$u_0 = s + u_{fs} \qquad (26)$$

This shortening can be calculated from a reference point x_0, which has zero axial displacement, by means of the following integral,

$$u_{fs}(x) = -\frac{1}{2}\int_{x_0}^{x} \left(v_0'\right)^2 dx \qquad (27)$$

This expression comes from the projection on the *x* axis of the difference between the undeformed length *dx* and the deformed length of arc $ds = \sqrt{1+v_0'^2}\,dx$. Substituting the longitudinal displacement of Eq. (26) into Eq. (15), yields the following expression for the elastic potential,

$$U = \frac{1}{2}\int_0^L EA\left(s'\right)^2 dx + \frac{1}{2}\int_0^L EI\left(v_0''\right)^2 dx \qquad (28)$$

It is observed that the elastic energy has the same form as in the linear formulation, although the meaning is different. The stiffness matrix is the same as the one used for the linear case $\mathbf{K}_L$, and so happens with the elastic forces. Therefore, the stiffening effect does not appear now in the elastic forces: it is translated to the inertia and constraint forces, since the foreshortening is introduced at kinematics level.

In order to calculate the total foreshortening on a finite element, the nodal displacement must be modified so that,

$$\boldsymbol{\delta}_0^e = \begin{pmatrix} u_0 \\ v_0 \end{pmatrix} = \begin{pmatrix} \mathbf{S}_l^e \\ \mathbf{S}_t^e \end{pmatrix}\mathbf{q}_f^e + \begin{pmatrix} u_{fs}^e \\ 0 \end{pmatrix} \qquad (29)$$

where u_{fs}^e is the foreshortening produced in that finite element by its own deflection, and can be calculated by applying Eq. (27) over the whole length of the element, L^e. Substituting v_0' by its interpolation,

$$u_{fs}^e = -\frac{1}{2}\int_0^{L^e} \mathbf{q}_f^{eT}\,\frac{\partial \mathbf{S}_t^{eT}}{\partial x}\,\frac{\partial \mathbf{S}_t^e}{\partial x}\mathbf{q}_f^e\,dx = -\frac{1}{2}\mathbf{q}_f^{eT}\mathbf{H}^e\mathbf{q}_f^e \qquad (30)$$

The shortening suffered by one element is then a quadratic function of the nodal coordinates, where $\mathbf{H}^e$ is a constant matrix depending only on the transversal interpolation functions and the length of the element.

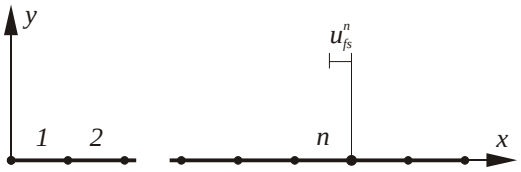

Fig. 2. Accumulated foreshortening at element *n*.

The total shortening accumulated by the finite elements located between the reference node (with zero axial displacement) and the finite element *n*, itself included, is the sum of all the element-level shortenings, as shown in figure 2,

$$u_{fs}^n = -\frac{1}{2}\sum_{e=1}^{n} \mathbf{q}_f^{eT} \mathbf{H}^e \mathbf{q}_f^e \tag{31}$$

This expression can be written in matrix form for each element, assembled for all the finite element coordinates of the beam, and then projected to the modal subspace,

$$u_{fs}^n = -\frac{1}{2}\mathbf{q}_f^T \mathbf{H}_{acc}^n \mathbf{q}_f = -\frac{1}{2}\mathbf{y}^T \mathbf{X}^T \mathbf{H}_{acc}^n \mathbf{X}\mathbf{y} = -\frac{1}{2}\mathbf{y}^T \mathbf{G}^n \mathbf{y} \tag{32}$$

If analytical functions are available for the modal shapes, these $\mathbf{G}^n$ matrices can be directly calculated by using the second expression of Eq. (20) to evaluate Eq. (27),

$$\mathbf{G}^n = \int_0^{L^n} \begin{Bmatrix} \phi_t'^1 \\ \vdots \\ \phi_t'^{ns} \\ \psi_t'^1 \\ \vdots \\ \psi_t'^{nd} \end{Bmatrix} \left\{ \phi_t'^1 \cdots \phi_t'^{ns} \ \psi_t'^1 \cdots \psi_t'^{nd} \right\} dx \tag{33}$$

where L^n is the length of the beam from the reference point to the end node (node *i*) of finite element *n*. If the modes are finite element displacement vectors, the integrals must be calculated by using the interpolation functions.

Therefore, the elastic displacement of node *i* is now,

$$\boldsymbol{\delta}_0^i = \mathbf{q}_f^i + \begin{Bmatrix} u_{fs}^n \\ 0 \end{Bmatrix} = \mathbf{X}^i \mathbf{y} + \begin{Bmatrix} u_{fs}^n \\ 0 \end{Bmatrix} = \mathbf{X}^i \mathbf{y} - \frac{1}{2}\begin{Bmatrix} 1 \\ 0 \end{Bmatrix} \mathbf{y}^T \mathbf{G}^n \mathbf{y} \tag{34}$$

Substituting this displacement into Eq. (3), and carrying out the time derivative results, for the nodal velocity,

$$\mathbf{v}^i = \dot{\mathbf{r}}_0 + \dot{\mathbf{A}}\left(\bar{\mathbf{r}}_u^i + \mathbf{X}_{fs}^i \mathbf{y}\right) + \mathbf{A}\left(\mathbf{X}_{fs}^i \dot{\mathbf{y}} + \dot{\mathbf{X}}_{fs}^i \mathbf{y}\right) \tag{35}$$

where $\mathbf{X}_{fs}$ is a variable matrix, which depends linearly on the modal amplitudes **y**,

$$\mathbf{X}_{fs}^i = \mathbf{X}^i - \frac{1}{2}\begin{bmatrix} 1 \\ 0 \end{bmatrix} \mathbf{y}^T \mathbf{G}^i \tag{36}$$

In order to implement the foreshortening in the equations of motion, the $\mathbf{G}^n$ accumulated shortening matrices must be first calculated and stored in a preprocessing stage. Then the new $\mathbf{X}_{fs}$ matrix, which is no longer constant, is calculated at every time-step and used to calculate matrix **B**, as it was done in Eq. (8)

These changes affect to the mass matrix, the velocity-dependent and applied force vectors. Moreover, those constraints involving nodes undergoing foreshortening must also be modified, since transversal modes affect the beam length. Therefore, the geometric stiffening effect is considered now through inertia and constraint forces, instead of through the elastic forces, as happened in the first and second nonlinear formulations.

IV. Test Model and Results

The model used is a typical example of geometric stiffening [2], [3], [4], [5], a 2D beam articulated at one of its ends, with the following characteristics: length, L=10 m; cross-sectional area, A=4,0·10^{-4} m^2; second moment of area, I=2,0·10^{-7} m^4; density, ρ=3000 Kg/m^3; Young modulus: E= 7,0·10^{10} N/m^2. The effect of gravity is neglected, and the beam spins an angle $\theta(t)$ around the articulation,

$$\theta = \begin{cases} \dfrac{\omega_s}{T_s}\left(\dfrac{t^2}{2} + \left(\dfrac{T_s}{2\pi}\right)\left[\cos\left(\dfrac{2\pi t}{T_s}\right) - 1\right]\right) & 0 \le t \le T_s \\ \omega_s\left(t - \dfrac{T_s}{2}\right) & T_s \le t \end{cases} \tag{37}$$

The time history of the in-plane tip deflection in local coordinates is recorded for T_s=15 s and ω_s=6 rad/s.

The beam is modelled with 10 finite elements, one transversal static mode and two transversal dynamic modes. A reference solution has been calculated with a global, finite-element based formulation, the ANCF [1], [6], which uses absolute positions and slopes as coordinates in a global inertial reference frame. This formulation applies nonlinear strain-displacement relationships so capturing all nonlinear effects, including geometric stiffening. In the simulation of reference, 15 elements were used.

The results obtained through the different formulations are discussed in the following subsections.

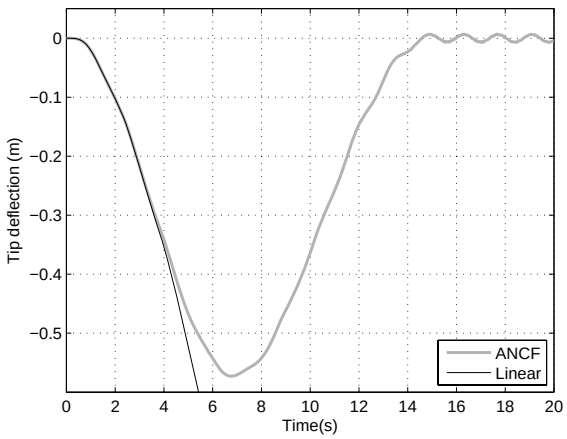

Fig. 3. Linear vs. ANCF.

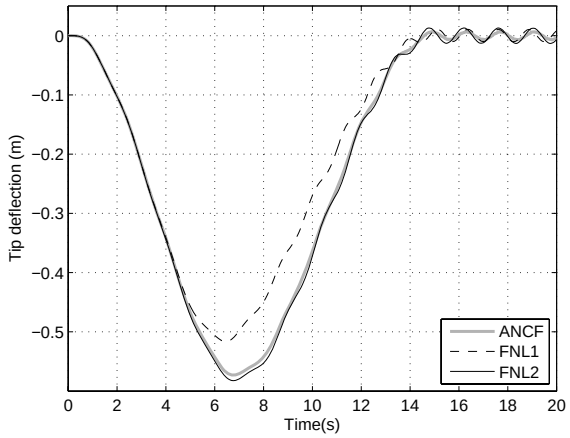

Fig. 4. First nonlinear formulation vs. ANCF.

A. *Linear formulation*

The linear formulation cannot account for the geometric stiffening effect. As it can be seen in figure 3, the tip deflection increases indefinitely because there is no coupling between axial and transversal displacements.

B. *First nonlinear formulation*

This formulation needs to include at least one axial mode, as the geometric stiffness matrix depends on the axial deformation. In the example, the axial displacement, caused by centrifugal forces, has a nonlinear distribution, so that the first dynamic axial mode is required to achieve reasonable accuracy. Figure 4 shows that using only one linear static mode (FNL1 curve) yields unacceptable results. Therefore, two axial modes are needed at least to correctly simulate the motion of the beam (FNL2 curve).

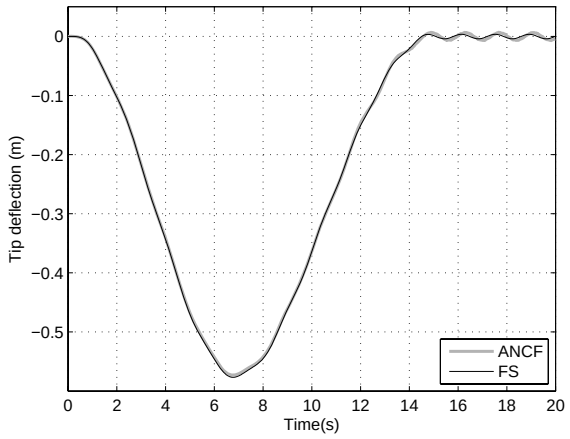

Fig. 5. Foreshortening formulation vs. ANCF.

C. *Foreshortening formulation*

The foreshortening formulation (FS curve in figure 5) achieves the best results, despite the absence of axial modes. The quality of the correlation becomes more obvious at the steady-state stage, where the first nonlinear formulation shows a higher oscillation amplitude.

D. *Efficiency comparison*

The following table shows the CPU-times for all the simulations, run with the same integrator and parameters, with a time-step of 0,01 s. The formulations are sorted by accuracy: first nonlinear with one axial mode (FNL1), first nonlinear with two axial modes (FNL2), and foreshortening (FS). The ANCF, several orders of magnitude slower, has not been included in the table.

Formulation	FNL1	FNL2	FS
Time (s)	11,03	12,96	10,13

TABLE I. CPU-times for all the formulations.

V. Conclusions

As has been shown in the tests, the linear formulation yields incorrect results, what means that any of the higher order formulations must be used. The first nonlinear formulation is very easy to implement, but presents some problems, since only one axial mode is not sufficient for obtaining accurate results, and the use of axial modes of high natural frequencies hinders the integration process. The foreshortening formulation has proven to be the fastest and also the most accurate. It doesn't require the use of axial modes, although they could be added in case that axial stresses were needed.

References

[1] Shabana, A.A., *Dynamics of Multibody Systems, 2nd Edition*, Cambridge, Cambridge University Press, 1998.

[2] Kane, T.R., Ryan, R.R., Banerjee, A.K. Dynamics of a cantilever beam attached to a moving base. *AIAA Journal*. 10(2):139-151, 1987.

[3] Mayo, J.M., Domínguez, J. and Shabana, A.A. Geometrically nonlinear formulations of beams in flexible multibody dynamics. *Journal of Vibration and Acoustics*, 117:501-509, 1995.

[4] Mayo, J.M., García, D. and Domínguez, J. Study of the geometric stiffening effect: comparison of different formulations. *Multibody System Dynamics*, 11:321-341, 2004.

[5] Sharf, I. Geometrically non-linear beam element for dynamics simulation of multibody systems. *International Journal for Numerical Methods in Engineering*. 39:763-786, 1996.

[6] Omar, M.A. and Shabana, A.A. A two-dimensional shear deformable beam for large rotation and deformation problems. *Journal of Sound and Vibration*. 243:565-576, 2001.

[7] Cuadrado, J., Gutiérrez, R. Naya, M.A. and González, M. Experimental validation of a flexible MBS dynamic formulation through comparison between measured and calculated stresses on a prototype car. *Multibody System Dynamics*. 11:147-166, 2004.

[8] Géradin, M. and Cardona, A. *Flexible Multibody Dynamics – A Finite Element Approach.* John Wiley and Sons, 2001.

[9] Craig, R.R. and Bampton, M.C.C. Coupling of substructures for dynamic analyses. *AIAA Journal*, 6(7):1313-1319, 1968.